

# Galactic Dynamics via General Relativity: A Compilation and New Developments

F. I. Cooperstock and S. Tieu

Department of Physics and Astronomy, University of Victoria  
P.O. Box 3055, Victoria, B.C. V8W 3P6 (Canada)

Email: cooperst@uvic.ca, stieu@uvic.ca

August 21, 2018

## Abstract

We consider the consequences of applying general relativity to the description of the dynamics of a galaxy, given the observed flattened rotation curves. The galaxy is modeled as a stationary axially symmetric pressure-free fluid. In spite of the weak gravitational field and the non-relativistic source velocities, the mathematical system is still seen to be non-linear. It is shown that the rotation curves for various galaxies as examples are consistent with the mass density distributions of the visible matter within essentially flattened disks. This obviates the need for a massive halo of exotic dark matter. We determine that the mass density for the luminous threshold as tracked in the radial direction is  $10^{-21.75} \text{ kg}\cdot\text{m}^{-3}$  for these galaxies and conjecture that this will be the case for other galaxies yet to be analyzed. We present a velocity dispersion test to determine the extent, if of any significance, of matter that may lie beyond the visible/HI region. Various comments and criticisms from colleagues are addressed.

## 1 Introduction

This paper presents a unified amalgam of our work to date in [1], [2], [3] and the expansion of the Letter [4] as well as further progress in the application of general relativity to galactic dynamics. The motivation for the work stems from the need to account for the observed essentially flat velocity rotation curves for galaxies. This has been a central issue in astrophysics. There has been much speculation

over the question of the nature of the dark matter that is believed to be required for the consistency of the observations of higher than expected stellar velocities with Newtonian gravitational theory. While various researchers are now turning to gravitational lensing in the search for evidence for dark matter, probably the majority of researchers regard the flat galactic rotation curves as the key indicators. Clearly the issue is of paramount importance given that the dark matter is said to comprise the dominant constituent of an extended galactic mass by multiple factors [5]. The dark matter enigma has served as a spur for particle theorists to devise acceptable candidates for its constitution. While physicists and astrophysicists have pondered over the problem, other researchers have devised new theories of gravity to account for the observations (see for example [6, 7, 8, 9]). However the latter approaches, imaginative as they may be, have met with understandable skepticism, having been devised solely for the purpose of the task at hand. To our knowledge, general relativity has never previously been proposed as a possible means of accounting for the flat rotation curves without invoking large stores of dark matter. However, general relativity remains the preferred theory of gravity with Newtonian theory as its limit where appropriate. General relativity has been successful in every test that it has encountered, going beyond Newtonian theory where required. Therefore, should it actually transcend Newtonian gravity in resolving the problem at hand, it would greatly alter the understanding of some basic aspects in physics. In what follows, we will set out to show that this is the case.

It is understandable that the conventional gravity approach has focused upon Newtonian theory in the study of galactic dynamics as the galactic field is weak (apart from the deep core regions where black holes are said to reside, at least in some galaxies) and the motions are non-relativistic ( $v \ll c$ ). It was this approach that led to the inconsistency between the theoretical Newtonian-based predictions and the observations of the visible sources alone. To reconcile the theory with the observations, researchers subsequently concluded that to realize the observed motions, dark matter must be present around galaxies in vast massive halos that constitute the great bulk of the extended galactic masses<sup>1</sup>. While this might at first sight appear to be a relatively simple cure to the problem of motion, these massive halos cannot be identified with any known form of matter, hence our use of the adjective “exotic” to describe this presumed matter. However, in dismissing general relativity in favor of Newtonian gravitational theory for the study of galactic dynamics, insufficient attention has been paid to the fact that the stars that compose the galaxies are essentially in motion under gravity alone (“gravitationally bound”). It has been known since the time of Eddington that the gravita-

---

<sup>1</sup>See however [34] who argues for a much less massive halo based upon gravitational lensing data.

tionally bound problem in general relativity is an intrinsically non-linear problem<sup>2</sup> even when the conditions are such that the field is weak and the motions are non-relativistic, at least in the time-dependent case. *Most significantly, we have found that under these conditions, the general relativistic analysis of the problem is also non-linear for the stationary (non-time-dependent) case at hand.* Thus the intrinsically linear Newtonian-based approach used to this point has been inadequate for the description of the galactic dynamics and Einstein’s general relativity must be brought into the analysis within the framework of established gravitational theory<sup>3</sup>. This is an essential departure from conventional thinking on the subject and it leads to major consequences as we discuss in what follows. We will demonstrate that via general relativity, what we will refer to as “generating” potentials producing the observed flattened rotation curves can be linked to the mass density distributions of the essentially flattened disks, obviating any necessity for dominant massive exotic dark matter halos in the total extended galactic composition.

We will also present the indicator that the threshold for luminosity, as we probe in the radial direction, occurs at a density of  $10^{-21.75} \text{ kg}\cdot\text{m}^{-3}$ .

Since our initial posting [1], many colleagues have offered their comments and criticisms which we address in Section 4. Some of these issues have already been discussed in [2], [3] and [4]. In this paper, we expand upon our discussions of the various papers. We also focus upon a new observational discriminator for assessing the degree, if any, of external matter that may lie beyond the visible/HI regions.

## 2 The Model Galaxy

Within the context of Newtonian theory, Mestel [10] considered a special rotating disk with surface density inversely proportional to radius. Using a disk potential with Bessel functions that we will also use in what follows but in quite a different manner, he found that it leads to an absolutely flat galactic rotation velocity curve.<sup>4</sup> Interestingly, the gradient of the potential in this, as in all Newtonian treatments, relates to acceleration whereas in the general relativistic treatment,

---

<sup>2</sup>It is to be noted that after nearly a century of research, there still does not exist a closed-form solution of the two-body problem in general relativity.

<sup>3</sup>Actually within the framework of Newtonian theory, it is possible to define an “effective” potential (see for example [5] page 136) to incorporate the centrifugal acceleration in a rotating coordinate system with a given angular velocity. Since this contains the square of the angular velocity of the rotating frame, there is already the hint of non-linearity present. However, in what follows in general relativity, we will see the non-linearity related to the angular velocity as a *variable* function. Moreover, for a system in rotation, this non-linearity cannot be removed globally.

<sup>4</sup>This is also the case for the MOND [6, 7, 8] model.

we will show that the gradient of a generating potential gives the stellar tangential velocity (14).

When we consider the complexity of the detailed structure of a spiral galaxy With its arms and irregular density variations, it becomes clear that the modeling within the context of the complicated theory of general relativity must entail some simplifications. As long as the essence of the structure is captured, these simplifications are justified and valuable information can be gleaned. Thus, in terms of its essential characteristics, we consider a uniformly rotating fluid without pressure and symmetric about its axis of rotation. We do so within the context of general relativity. The stationary axially symmetric metric can be described in generality in the form

$$ds^2 = -e^{\nu-w}(udz^2 + dr^2) - r^2e^{-w}d\phi^2 + e^w(cdt - Nd\phi)^2 \quad (1)$$

where  $u$ ,  $\nu$ ,  $w$  and  $N$  are functions of cylindrical polar coordinates  $r$ ,  $z$ . It is easy to show that to the order required,  $u$  can be taken to be unity.<sup>5</sup> It is most simple to work in the frame that is co-moving with the matter,

$$U^i = \delta_0^i \quad (2)$$

where  $U^i$  is the four-velocity<sup>6</sup>. This was done in the pioneering paper by van Stockum [11] who set  $w = 0$  from the outset<sup>7</sup>. As in [12], and following [13], we perform a purely *local* ( $r, z$  held fixed at each point when taking differentials) transformation<sup>8</sup>

$$\bar{\phi} = \phi + \omega(r, z) t \quad (3)$$

that locally diagonalizes the metric. In this manner, we are able to deduce the local angular velocity  $\omega$  and the tangential velocity  $V$  as

$$\omega = \frac{Nce^w}{r^2e^{-w} - N^2e^w} \approx \frac{Nc}{r^2} \quad (4)$$

$$V = \omega r \quad (5)$$

---

<sup>5</sup>Retaining terms of non-zero order in  $G$  for  $u$  induces terms of order  $G^n$  with  $n > 1$  in the field equations.

<sup>6</sup>This is reminiscent of the standard approach that is followed for FRW cosmologies. However, the FRW spacetimes are homogeneous and they are not stationary.

<sup>7</sup>Interestingly, the geodesic equations imply that  $w = \text{constant}$  (which can be taken to be zero as in [11]) even for the *exact* Einstein field equations as studied in [11]. In fact the requirement that  $w = 0$  can be seen directly using (2) and the metric equation  $g_{ik}U^iU^k = 1$  [2].

<sup>8</sup>Note that this local transformation is used only to deduce the connection between  $N$  and  $\omega$  (and hence  $V$ ). All subsequent work continues in the original unbarred co-moving frame.

with the approximate value applicable for the weak fields under consideration. The Einstein field equations to order  $G^1$  with  $w$  retained for later comparison, are<sup>9</sup>

$$\begin{aligned}
2r\nu_r + N_r^2 - N_z^2 &= 0, \\
r\nu_z + N_r N_z &= 0, \\
N_r^2 + N_z^2 + 2r^2(\nu_{rr} + \nu_{zz}) &= 0, \\
N_{rr} + N_{zz} - \frac{N_r}{r} &= 0,
\end{aligned} \tag{6}$$

$$\begin{aligned}
&\left(w_{rr} + w_{zz} + \frac{w_r}{r}\right) + \frac{3}{4}r^{-2}(N_r^2 + N_z^2) \\
&+ \frac{N}{r^2}\left(N_{rr} + N_{zz} - \frac{N_r}{r}\right) - \frac{1}{2}(\nu_{rr} + \nu_{zz}) = 8\pi G\rho/c^2
\end{aligned} \tag{7}$$

where  $G$  is the gravitational constant and  $\rho$  is the mass density. Subscripts denote partial differentiation with respect to the indicated variable. These equations are easily combined to yield

$$\nabla^2 w + \frac{N_r^2 + N_z^2}{r^2} = \frac{8\pi G\rho}{c^2} \tag{8}$$

where the first term is the flat-space Laplacian in cylindrical polar coordinates

$$\nabla^2 w \equiv w_{rr} + w_{zz} + \frac{w_r}{r} \tag{9}$$

and  $\nu$  would be determined by quadratures.

With the freely gravitating constraint and the requirement that  $w = 0$  arising from the choice of co-moving coordinates, the field equations for  $N$  and  $\rho$  in this globally dust distribution are reduced to<sup>10</sup>

$$N_{rr} + N_{zz} - \frac{N_r}{r} = 0 \tag{10}$$

$$\frac{N_r^2 + N_z^2}{r^2} = \frac{8\pi G\rho}{c^2}. \tag{11}$$

Note that from both the field equation for  $\rho$  and the expression for  $\omega$  that  $N$  is of order  $G^{1/2}$ . The non-linearity of the galactic dynamical problem is manifest

---

<sup>9</sup>This is a loose notation favored by many relativists but adequate for our purposes here as a smallness parameter.

<sup>10</sup>Note that with the minus sign in (10),  $N$  does not satisfy the Laplace equation.

through the non-linear relation<sup>11</sup> between the functions  $\rho$  and  $N$ . Rotation under freely gravitating motion is the key here. By contrast, for time-independence in the non-rotating problem, there must be pressure present to maintain a static configuration (hence altering the right hand side of (6)),  $N$  vanishes for vanishing  $\omega$  and  $\nabla^2 w$  is non-zero yielding the familiar Poisson equation of Newtonian gravity. In the present case, it is the *rotation* via the function  $N$  that connects directly to the density and the now non-linear equation is in sharp contrast to the linear Poisson equation.

Interestingly, (10) can be expressed as

$$\nabla^2 \Phi = 0 \tag{12}$$

where

$$\Phi \equiv \int \frac{N}{r} dr \tag{13}$$

and hence flat-space harmonic functions  $\Phi$  are the generators of the axially symmetric stationary pressure-free weak fields that we seek<sup>12</sup>. These are the generating potentials referred to earlier. It is to be noted that these generating potentials play a different role in general relativity than do the potentials of Newtonian gravitational theory even though both functions are harmonic. Using (5) and (13), we have the expression for the tangential velocity of the distribution

$$V = c \frac{N}{r} = c \frac{\partial \Phi}{\partial r} \tag{14}$$

### 3 Modeling the Observed Galactic Rotation Curves

Since the field equation for  $\rho$  is non-linear, the simpler way to proceed in galactic modeling is to first find the required generating potential  $\Phi$  and from this, derive an appropriate function  $N$  for the galaxy that is being analyzed. With  $N$  found, (11) yields the density distribution. If this is in accord with observations, the efficacy of the approach is established. This is in the reverse order of the standard approach to solving gravitational problems but it is most efficient in this formalism because of the existence of one linear field equation.

---

<sup>11</sup>While we have eliminated  $w$  either by using the geodesic equations to get (11) or by the metric equation and the choice of co-moving coordinates,  $N$  cannot be eliminated and hence non-linearity is intrinsic to the study of the galactic dynamics.

<sup>12</sup>In fact Winicour [35] has shown that all such sources, even when the fields are strong, are generated by such flat-space harmonic functions.

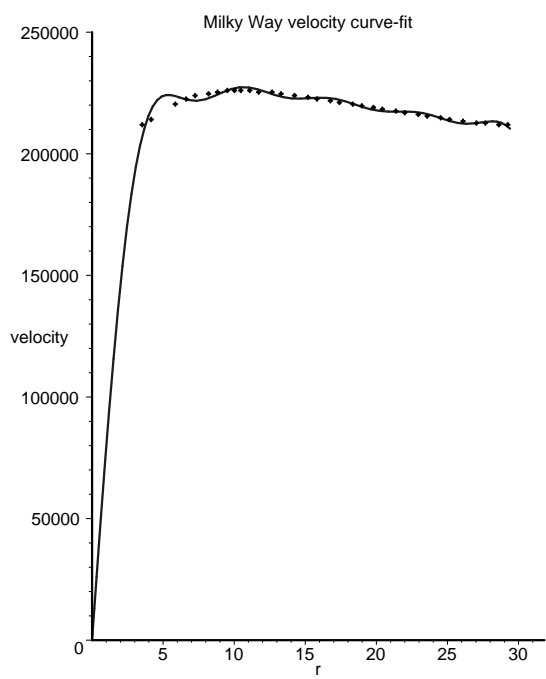


Figure 1: Velocity curve-fit for the Milky Way in units of m/s vs Kpc.

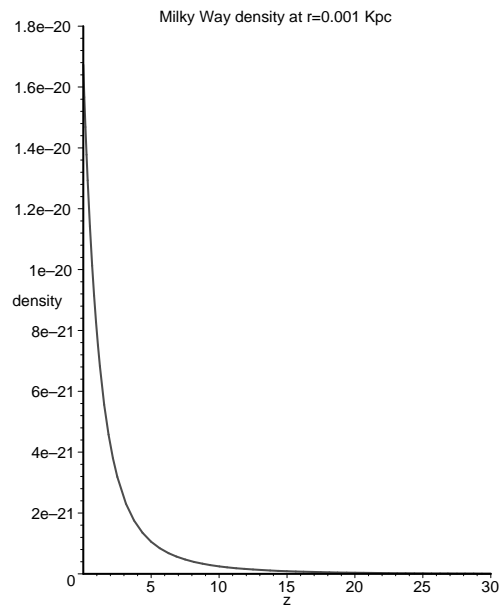
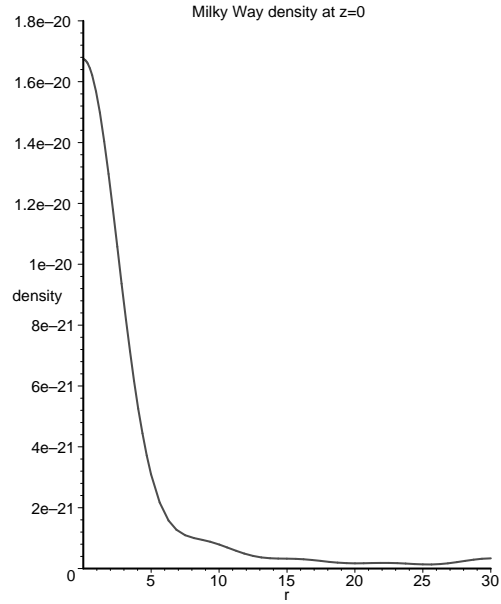


Figure 2: Derived density profiles in units of  $\text{kg}/\text{m}^3$  for the Milky Way at (a)  $z = 0$  and (b)  $r = 0.001$  Kpc.



Every galaxy is different and each requires its own composing elements to build the generating potential. In cylindrical polar coordinates, separation of variables yields the following solution for  $\Phi$  in (12):

$$\Phi = Ce^{-k|z|}J_0(kr) \quad (15)$$

where  $J_0$  is the Bessel function  $m = 0$  of Bessel  $J_m(kr)$  and  $C$  is an arbitrary constant.<sup>13</sup> We use the linearity of (12) to express the general solution of this form as a linear superposition

$$\Phi = \sum_n C_n e^{-k_n|z|} J_0(k_n r) \quad (16)$$

with  $n$  chosen appropriately for the desired level of accuracy. From (16) and (14), the tangential velocity<sup>14</sup> is

$$V = -c \sum_n k_n C_n e^{-k_n|z|} J_1(k_n r) \quad (17)$$

With the  $k_n$  chosen so that the  $J_0(k_n r)$  terms are orthogonal<sup>15</sup> to each other, we have found that only 10 functions with parameters  $C_n$ ,  $n \in \{1 \dots 10\}$  suffice to provide an excellent fit<sup>16</sup> to the velocity curve for the Milky Way. The details are provided in the Appendix and the curve fit is shown in Figure 1.<sup>17</sup> From (14) and (17), the  $N$  function is determined in detail and from (11), the density distribution follows. This is shown in Figure 2 as a function of  $r$  at  $z = 0$  as well as a function of  $z$  at  $r = 0.001$  Kpc. We see that the distribution is an essentially flattened disk with good correlation with the observed overall averaged density

---

<sup>13</sup>See for example [36]. With this form of solution, the absolute value of  $z$  must be used to provide the proper reflection of the distribution for negative  $z$ . While this produces a discontinuity in  $N_z$  at  $z = 0$ , it is important to note that in the problem at hand, this discontinuity is consistent with the general case of having a density gradient discontinuity at the plane of reflection symmetry. This point is discussed further in the text.

<sup>14</sup> $dJ_0(x)/dx = -J_1(x)$  from [37].

<sup>15</sup>Just as the  $\sin kx$  functions are orthogonal for integer  $k$ , the Bessel functions  $J_0(kr)$  have their own orthogonality relation:  $\int_0^1 J_0(k_n r) J_0(k_m r) r dr \propto \delta_{mn}$  where  $k_n$  are the zeros of  $J_0$  at the limits of integration. This orthogonality condition is on  $\Phi$  rather than on  $V$  because the differential equation dictates the integral condition.

<sup>16</sup>It should be noted that unlike typical velocity curve fits that allow arbitrary velocity functions, our curve fits are constrained by the demand that they be created from derivatives of harmonic functions.

<sup>17</sup>Note that the  $J_1(x)$  Bessel functions are 0 at  $x = 0$  and oscillate with decreasing amplitude, falling as  $1/\sqrt{x}$  asymptotically [37]. However, this feature alone does not assure a realistic fall-off of matter. This issue is addressed in Section 4. Also, the present curves drop as  $r$  approaches 0. This is in contrast to the Mestel [10] and MOND [6, 7, 8] curves that are flat everywhere.

data for the Milky Way (see Figure 3).<sup>18</sup> The integrated mass is found to be  $21 \times 10^{10} M_{\odot}$  which is at the lower end of the estimated mass range of  $20 \times 10^{10} M_{\odot}$  to  $60 \times 10^{10} M_{\odot}$  as established by various researchers. It is to be noted that the approximation scheme would break down in the region of the galactic core should the core harbor a black hole or even a naked singularity (see e.g. [14]). *Most significantly, our correlation of the flat velocity curve is achieved with disk mass of an order of magnitude smaller than the envisaged halo mass of exotic dark matter.*<sup>19</sup>

General relativity does not distinguish between the luminous and non-luminous contributions. The deduced  $\rho$  density distribution is derived from the totality of the two. Any substantial amount of non-luminous matter (i.e. *conventional* non-exotic dark matter) would necessarily lie in the flattened region relatively close to  $z = 0$  because this is the region of significant  $\rho$  and would be due to dead stars, planets, neutron stars and other normal non-luminous baryonic matter debris. Each term within the series has  $z$ -dependence of the form  $e^{-k_n|z|}$  which causes the steep density fall-off profile as shown in Figure 2(b). This fortifies the picture of a standard galactic essentially flattened disk-like shape as opposed to a halo sphere. From the evidence provided thus far by rotation curves<sup>20</sup>, there is no support for the widely accepted notion of the necessity for massive halos of exotic dark matter surrounding visible galactic disks: conventional gravitational theory, namely general relativity, can account for the observed flat galactic rotation curves linked to essentially flattened disks with no evident need for exotic dark matter.

We have also performed curve fits for the galaxies NGC 3031, NGC 3198 and NGC 7331. The data are provided in the Appendix and the remarkably precise velocity curve fits are shown in Figures 4 to 6 where the density profiles are presented for  $r$  at  $z = 0$ . Again the picture is consistent with the observations and the mass is found to be  $10.1 \times 10^{10} M_{\odot}$  for NGC 3198. This can be compared to the result from Milgrom's [6, 7, 8] modified Newtonian dynamics of  $4.9 \times 10^{10} M_{\odot}$  and the value given through observations (with Newtonian dynamics) by Kent [15] of  $15.1 \times 10^{10} M_{\odot}$ . While the visible light profile terminates at  $r = 14$  Kpc, the HI profile extends to 30 Kpc. If the density is integrated to 14 Kpc, it yields a mass-to-light ratio of  $7Y_{\odot}$ . However, integrating through the HI outer region to  $r = 30$  Kpc yields  $14Y_{\odot}$  using data from [16].

For NGC 7331, we calculate a mass of  $26.0 \times 10^{10} M_{\odot}$ . Kent [15] finds a value

---

<sup>18</sup>In Figure 3, we see that in the cross-sectional density plot, the equidensity contours are approximately elliptical around the visible galactic region.

<sup>19</sup>See e.g.[38, 39] for proposed values of extended halo masses. See also our discussions in Sections 4 and 5 of the added mass in extended dust distributions.

<sup>20</sup>See Section 5 for a proposed observational test for assigning a measure of mass to the region extending beyond the visible/HI region.

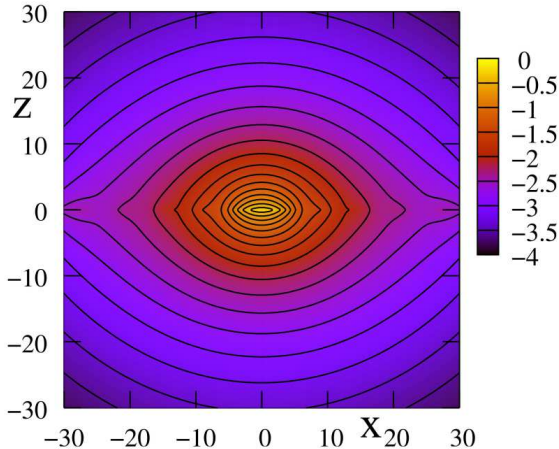


Figure 3: Cross-sectional density contour plot for the Milky Way model.

of  $43.3 \times 10^{10} M_{\odot}$ . For NGC 3031, the mass is calculated to be  $10.9 \times 10^{10} M_{\odot}$  as compared to Kent's value of  $13.3 \times 10^{10} M_{\odot}$ . Our masses are consistently lower than the masses projected by models invoking exotic dark matter halos and our distributions roughly tend to follow the contours of the optical disks.

It is interesting to note that from the figures provided by Kent [15] for optical intensity curves and our log density profiles for NGC 3031, NGC 3198 and NGC 7331, we determine that the threshold density for the onset of visible galactic light as we probe in the radial direction is at  $10^{-21.75} \text{ kg}\cdot\text{m}^{-3}$  (Figure 7 and Figure 8). It would be of interest to explore as many sources as possible to test the indicated hypothesis that this density is the universal optical luminosity threshold for galaxies as tracked in the radial direction. Alternatively, should this hypothesis be further substantiated, the radius at which the optical luminosity fall-off occurs can be predicted for other sources using this special density parameter. The predicted optical luminosity fall-off for the Milky Way is at a radius of 19-21 Kpc based upon the density threshold indicator that we have determined.

Various authors attempt to incorporate the Tully- Fisher law [17] into their modified theories of gravity. General relativity can provide an equivalent albeit considerably more complicated relation but in integral form. From (10) and (14), the radial gradient of the galactic mass can be expressed in terms of velocity as

$$M_r(r) = \frac{1}{2G} \int_0^{\infty} \left( r (V_r^2 + V_z^2) + \frac{V^2}{r} + 2VV_r \right) dz \quad (18)$$

and a doubling has been used to account for the lower disk contribution.

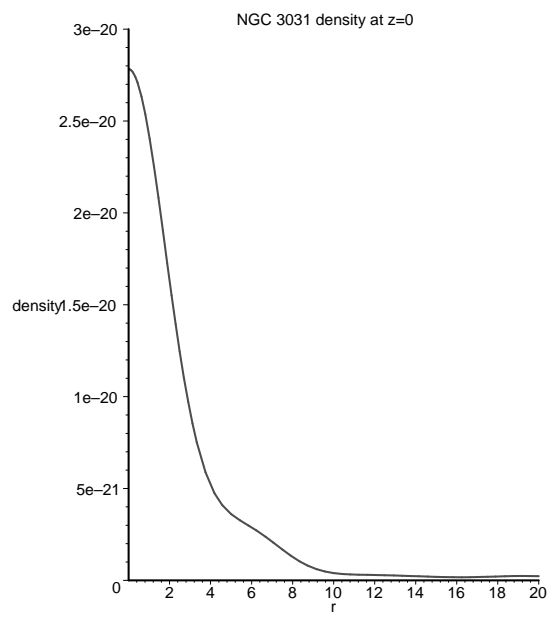
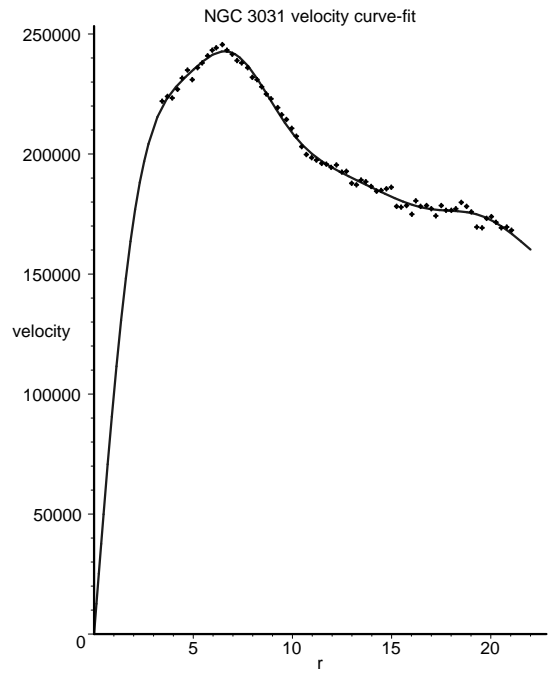


Figure 4: Velocity curve-fit and derived density for NGC 3031

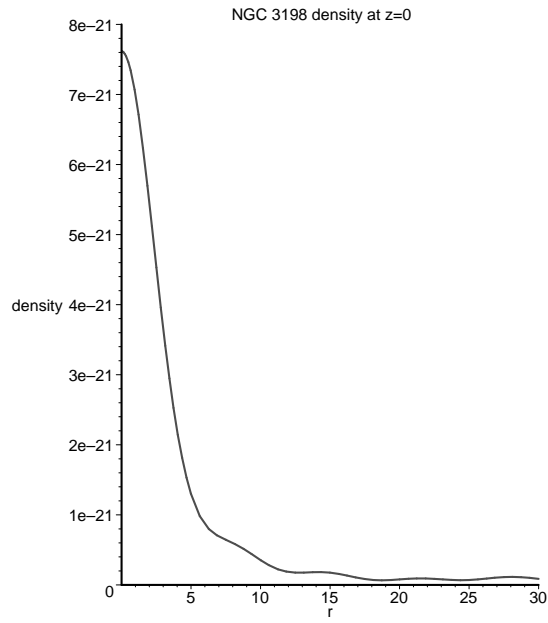
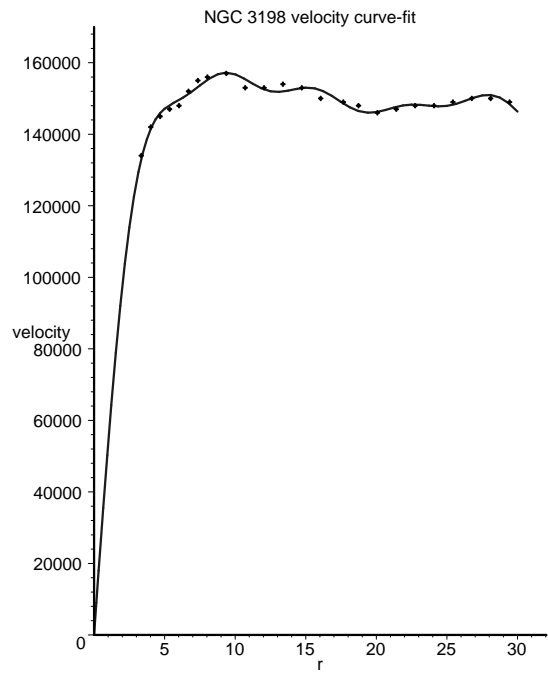


Figure 5: Velocity curve-fit and derived density for NGC 3198

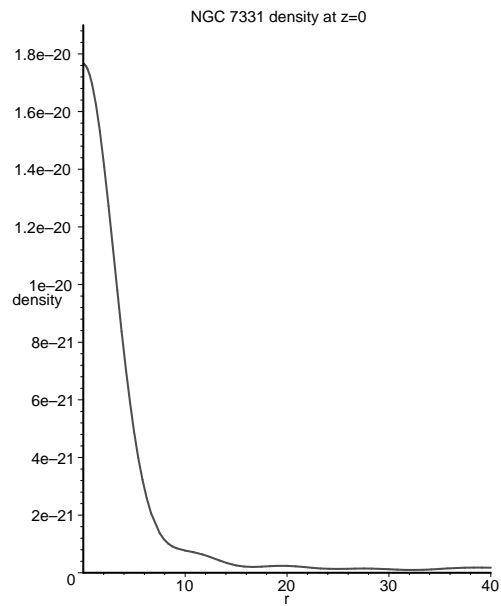
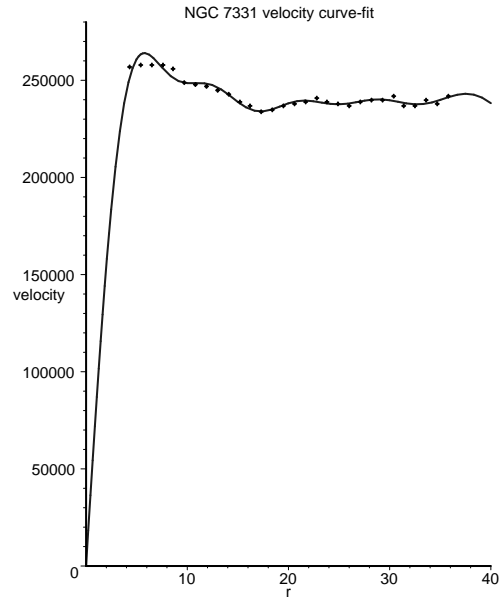


Figure 6: Velocity curve-fit and derived density for NGC 7331

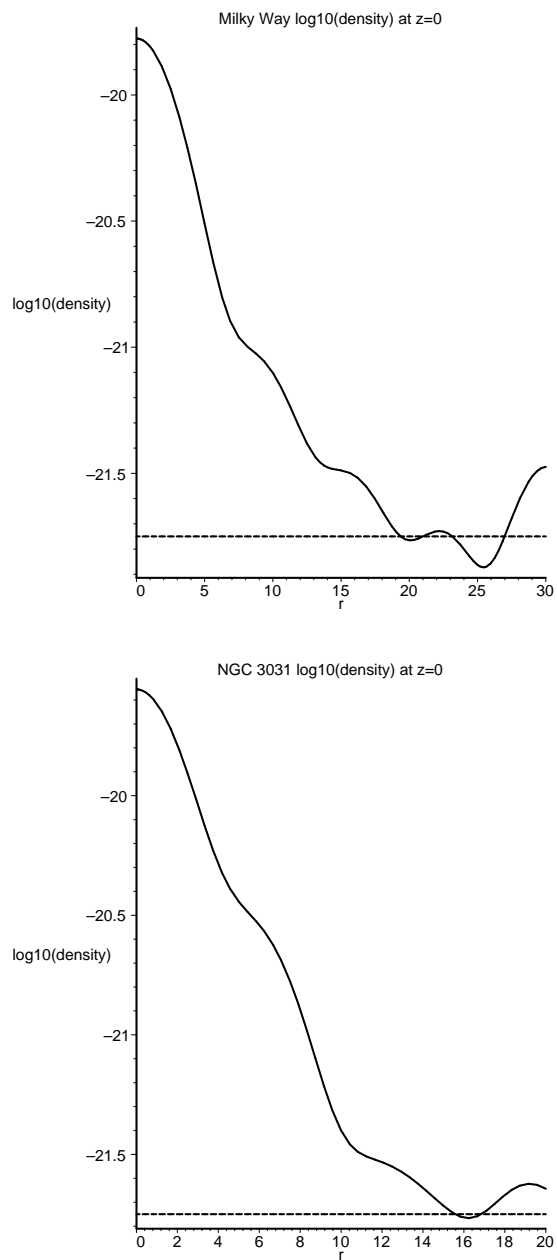


Figure 7: Log graphs of density for (a) the Milky Way and (b) NGC 3031 showing the density fall-off. The  $-21.75$  dashed line provides a tool to predict the outer limits of visible matter. The fluctuations at the end are the result of limited curve-fitting terms.

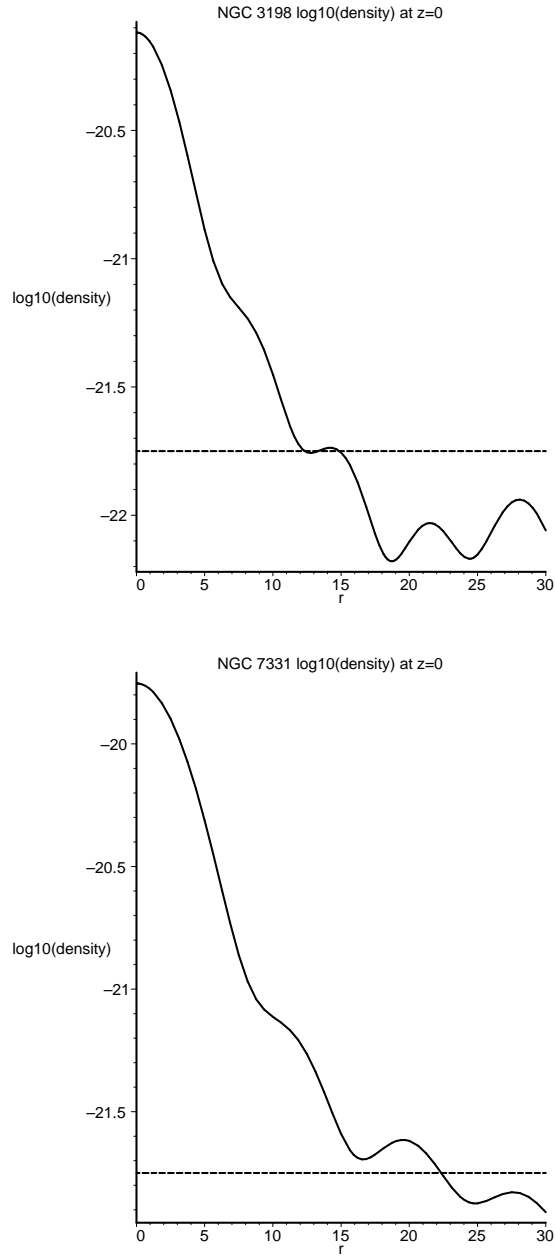


Figure 8: Log graphs of density for (a) the NGC 3198 and (b) NGC 7331 showing the density fall-off. The  $-21.75$  dashed line provides a tool to predict the limits of luminous matter. As before, there are fluctuations near the border.



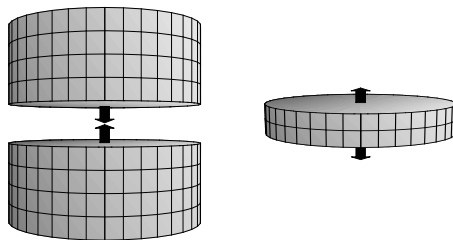


Figure 9: Normal vectors used to calculate flux

## 4 Replies to Various Analyses

Since the initial posting of our paper [1], there has been an interesting variety of critical papers as well as two papers lending support to our work [18] [19]. Some of the issues arising from these papers have been addressed in our companion paper [2], in [3] and in [4]. For completeness, in what follows we will reply to all of the most relevant papers to date in this section as well as the frequently asked questions and comments proffered by our colleagues.

An issue first raised privately to us by some colleagues and later in [20] [21] concerns the nature of the matter distribution. They have noted that given the existence of the discontinuity of  $N_z$  that we had pointed to in [1], a significant surface tensor  $S_i^k$  can be constructed with a surface density component given by

$$(8\pi G/c^2)S_t^t = \frac{N[N_z]}{2r^2} - \frac{[\nu_z]}{2} \quad (19)$$

to order  $G^1$ . The notation  $[\cdot]$  denotes the jump over a discontinuity of the given function, here at  $z = 0$ . Using (6), this becomes

$$(8\pi G/c^2)S_t^t = \frac{N[N_z]}{2r^2} + \frac{N_r[N_z]}{2r} \quad (20)$$

It was claimed that this necessarily implied the existence of a singular *physical* surface of mass in the galactic plane above and beyond the continuous mass distribution that we had found, thus rendering our model unphysical.

Having received this challenge, we calculated the surface mass that was said to be present in the four galaxies that we had studied by integrating (20) over the surface without paying heed to the actual sign of the result. Suspicions were aroused from the discovery that (20) in each case gave a numerical value slightly less than the mass that we had derived from the volume integral of our *continuous* mass density distribution using (17), (14) and (11).<sup>21</sup> This pointed to a plausible

---

<sup>21</sup>It should be noted that the two terms in (20) were found to contribute equally.

explanation: in our case, *with our choice of model*, there is no *physical* mass layer present on the  $z = 0$  plane. *The surface integral of this singular layer is merely a mathematical construct that indirectly describes most of the continuously distributed mass by means of the Gauss divergence theorem.* To see this, consider the vector  $\mathbf{F}$  defined as <sup>22</sup>

$$\mathbf{F} \equiv A(r, z)\mathbf{e}_r + B(r, z)\mathbf{e}_z \quad (21)$$

where

$$(8\pi G/c^2)B \equiv \frac{NN_z}{2r^2} + \frac{N_r N_z}{2r} \quad (22)$$

as a first option. We choose  $A(r, z)$  so that

$$\int \nabla \cdot \mathbf{F} dV \equiv (8\pi G/c^2)M \quad (23)$$

where  $M$  is the total mass. As a more transparent second option, we choose

$$(8\pi G/c^2)B \equiv \frac{NN_z}{r^2} \quad (24)$$

where we define

$$\nabla \cdot \mathbf{F} \equiv (8\pi G/c^2)\rho \quad (25)$$

From these definitions, we deduce the form of  $A(r, z)$  in order to produce the density as expressed through  $N$  in (11). We calculate the mass over the cylindrical volume defined by  $-\infty < z < \infty$ ,  $0 < r < r_{galaxy}$ . By the Gauss divergence theorem, the volume integral of  $\rho$ , via (25) is equal to the integral of the normal component of  $\mathbf{F}$  over the bounding surfaces. However, the integration must be over a continuous domain and since the  $\mathbf{e}_z$  component is discontinuous over the  $z = 0$  plane, the volume integral must be split into an upper and a lower half. The two new surface integrals together would constitute the jump integral of (20) in the first option if one were to be cavalier about the directions of unit *outward* normals, as we shall discuss in what follows. The surfaces above and below the galaxy give zero because of the exponential factors in  $z$  and the final small contribution comes from the cylinder wall via the  $A$  function.

In our solution, the actual *physical* distribution of mass is not in concentrated layers over bounding surfaces: the Gauss theorem gives the value of the *distributed* mass via equivalent purely mathematical surface constructs as we are familiar from elementary applications of this theorem. Physically, the density is well defined and continuous throughout, except on the  $z = 0$  plane. In fact the limits as

---

<sup>22</sup> $\mathbf{e}_r$  and  $\mathbf{e}_z$  are unit vectors in the  $r$  and  $z$  directions.

$z = 0$  is approached give the same finite values from above and below. While the field equations break down at  $z = 0$ , the density for a physically viable model is logically defined by this limit at  $z = 0$ . However, with the chosen form of solution, the density *gradient* in the  $z$  direction is discontinuous on the  $z = 0$  plane. This gradient undergoes a reversal for a galactic distribution with diminishing density in both directions away from the symmetry plane. It is most convenient to achieve this with an abrupt reversal as we have done. There is no indication that this choice alters the essential physics.

Thus we have shown via the Gauss divergence theorem, that the supposed surface layer is merely a re-expression of the integrals that constitute the *continuous volume distribution* of mass. Indeed if one were to reject this interpretation and insist that these surface integrals reveal additional mass in the form of a layer, then the Gauss theorem would indicate that this mass must be negative. Indeed various authors (e.g. [21] [22]) have referred to negative mass layers. However, as Bondi had emphasized in his writings, negative mass repels rather than attracts. Therefore we had set out to test the viability of the presence of such negative mass to see if repulsion rather than attraction was in evidence. We considered a test particle in our model that was comoving with the rotating dust apart from having a component of velocity  $U^z$  normal to the  $z = 0$  plane. The geodesic equation in the  $z$  direction reduces to

$$\frac{dU^z}{ds} = \frac{N_r N_z (U^z)^2}{2r} \quad (26)$$

We had computed the complete  $N$  series for the galaxy NGC7331 (see [1]). We then focused upon points in the range  $r = 0.1$  to 30 and points above the  $z = 0$  symmetry plane  $z = 0.001$  to 1 for the right hand side of (26). All of the points gave a negative value as expected for the  $z$  acceleration (i.e. attraction) of a particle in the region above the symmetry plane. However, if the  $z = 0$  surface actually harboured a *physical* negative mass surface layer, indeed one of numerical value comparable to the positive mass of the normal galactic distribution,<sup>23</sup> then at the very least, one would have expected to witness a *repulsion* of the particle

---

<sup>23</sup>In an interesting recent paper [22], the motion of a test particle for a different type of distribution was analyzed in the locally non-rotating frame produced via the transformation in (3). In this case, the  $z$  geodesic equation is dominated by  $\Gamma_{00}^z$  for non-relativistic particles. In [22], this term indicated that  $dU^z/ds$  was positive for  $z > 0$  and hence implied an apparent repulsion of the test particle. However, the geodesic equation should apply to particles of the dust itself since they are geodesic. These particles are at rest in the original frame and have only tangential velocity in the locally non-rotating frame. The local transformation should not alter their having no  $z$  velocity yet there is an apparent  $z$  acceleration. This is a contradiction which is resolved as follows: while we can use the local transformation to derive the local angular velocity (and hence tangential velocity) of the particles, it is not legitimate to take derivatives of the metric found after the local transformation has been applied in order to derive

as the test particle approached the boundary. The absence of this occurrence adds further support to our original model [1] as being free of surface layers of mass.

It is true that our choice of solution leads to a discontinuity in the  $z$ -derivative of  $N$  across the  $z = 0$  plane. This goes hand-in-hand with the physically natural density *gradient* discontinuity across the symmetry plane.<sup>24</sup> To see this, consider the essential characteristics of our model which consists of dust with reflection symmetry about the  $z = 0$  plane. The density naturally increases symmetrically as this plane is approached from above and from below with the same absolute value but opposite sign from symmetry. In all generality, the density gradient will be different from zero as this plane is approached and because of reflection symmetry, the gradient will of necessity be discontinuous<sup>25</sup>. It is only with delicate fine-tuning that this discontinuity can be avoided and this will be the case only if the density gradient is adjusted to be precisely zero as the  $z = 0$  plane is approached from above and below.

As an exercise in response to critical comments [2], we achieved this approximately by choosing  $\cosh(\kappa_n z)$  functions in place of exponential functions to span the region in a sandwich encompassing the symmetry plane and employing the usual exponential functions beyond this sandwich. This led to the issue of matching the  $N$  and  $N_z$  functions along the external/internal region joins and it was achieved by using many different  $k_n$  parameters for the external exponential func-

---

acceleration. The former usage simply reads off the required angular velocity to diagonalize the metric locally. No differentiation is required to do so. However, the latter usage would be legitimate only if the transformation would have been effected *without* constraints, in this case the constraint of holding  $r$  and  $z$  fixed. By holding these fixed to derive the new  $ds^2$ , we have metric tensor components that are correct as such only through a different transformation at each point. Hence there is an inherent discontinuity of transformation. In this manner, we recognize the derivative required to find  $dU^z/ds$  as being illegitimately applied, thus resolving the contradiction. This also brings into question the interpretation of the lack of a  $1/r$  term in  $g_{00}$  in the locally non-rotating frame for the same reason. The  $1/r$  issue is a global one yet the transformation that brought the metric to the form that is being used is a purely local one. By contrast, no such problem arises in studying test particle motion relative to the dust co-moving frame with the particle following the motion of the dust cloud apart from a  $z$  velocity component. The result is logical: for  $U^r$  and  $U^\phi$  being zero, acceleration occurs only for  $U^z$  different from zero (otherwise it would be part of the dust cloud and hence stationary) and the acceleration is independent of the sign of the velocity. Moreover, the acceleration is *negative* for  $z > 0$  and *positive* for  $z < 0$ . Thus, it is *attracted* to the central plane in both cases. We thank Professor W.B. Bonnor for bringing his paper to our attention.

<sup>24</sup>This is even more benign than the density discontinuity in the constant density Schwarzschild sphere solution.

<sup>25</sup>The density gradient is governed by the behavior of odd derivatives of  $N$  with respect to  $z$ . However, the density itself is governed by  $N_z^2$  (11) which has the same limit as  $z$  approaches 0 from above or below. Thus, we define the value of  $\rho$  at  $z = 0$  by this common limit and hence the singularity is removable.

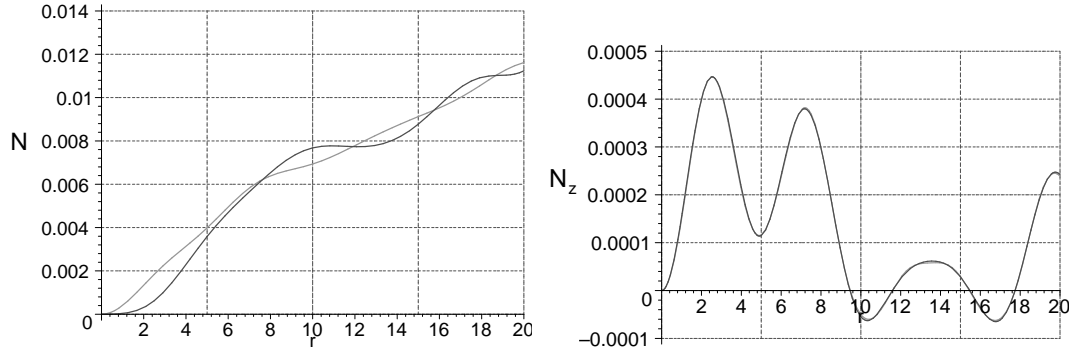


Figure 10: Matching conditions for  $N$  and  $\partial N/\partial z$  at  $z = z_0$ .

tions as opposed to the original 10 internal parameters of the original model. In [21], it was claimed that a matching could not be achieved but these authors had not realized that we used different and many parameters for the outside regions. Since then, we have refined the fit further by employing hundreds of external parameters and the improved fit is shown in Figure 10. However, it must be stressed that the generic situation would be one in which the density gradient is discontinuous at  $z = 0$ .

In [23], the well-known expression of the field equations in the harmonic gauge in Cartesian coordinates

$$\partial_k \partial^k h^{ab} = \frac{16\pi G}{c^4} \tau^{ab} \quad (27)$$

( $\tau^{ab}$  includes the energy-momentum tensor of the matter plus the non-linear terms in the Einstein equations) is invoked. (A related line of reasoning was followed in [20]). In [23], the author presents the standard description of the post-Newtonian perturbation scheme to conclude that the solution to the galactic problem must be the usual Newtonian one and that all corrections must be of higher order. Firstly, we did not use this scheme (as noted as well in [24]). Just as one would not logically choose Cartesian coordinates in the harmonic gauge to describe FRW cosmologies, one would not normally choose these for our stationary axially symmetric galactic problem. Our problem is greatly simplified with cylindrical polar coordinates co-moving with the matter. Secondly, for the gravitationally bound system under study, the metric components are of *different* orders in  $G$ <sup>26</sup>. If one were to take the approach suggested in [23], the equations (27) could be schematically expressed

---

<sup>26</sup>In general, first order perturbations lead to linear equations. However, there are situations where this is not the case. For example in fluid mechanics, certain approximations still lead to non-linear equations as in Burger's equation.

as

$$\nabla^2 h_{(1/2)} = 0, \quad \nabla^2 h_{(1)} = GT + h_{(1/2)}^2 \quad (28)$$

where tensorial superscripts have been suppressed and the lower case numbers refer to orders in  $G$ . In this manner, we would have incorporated the non-linear structure of our system within the framework of the scheme suggested by [23]. The novel aspect is that the lowest order equation (of order  $G^{1/2}$ ) in (28) has zero on the RHS and the second equation that would normally be the Newtonian Poisson equation, differs in that it has non-linear terms. Thus, the structure of our solution does not proceed as in the standard approach of (27). In the latter standard approach, the lowest order base solution is the Newtonian solution whereas in the galactic problem, the lowest order equation is the Laplace equation for which an order  $G^{1/2}$  solution is necessary (see [25] where this component is inappropriately chosen to be zero) and the next order (order  $G^1$ ) equation for the density (29),

$$\frac{N_r^2 + N_z^2}{r^2} = \frac{8\pi G\rho}{c^2} \quad (29)$$

has non-linear terms in the metric in the form of the squares of the derivatives of an order  $G^{1/2}$  metric tensor component  $N$ . Thus, our situation is unlike standard iterative perturbation scheme applications as envisaged in [23]. Hence there is no basis to draw the conclusions that are expressed therein.

Further in [23], the author refers to “extra matter” in the symmetry plane of the galaxy and muses whether our model “could be somehow fixed”. However, in [2] we presented the evidence that our solution embodies the physically natural density gradient discontinuity at the plane of symmetry and that it does not contain extra matter. Moreover, we showed that if there were to be a surface layer of mass, it would be negative mass but this was negated by the attraction rather than repulsion of test particles near the symmetry plane, as we discussed above.

The author concludes with an argument to attempt to provide dark matter through general relativity in the form of a geon where general relativity would be required and he deduces that this is impossible [23]. While we are in agreement with him that it is indeed impossible with geons (but from a different line of reasoning, see [26],[27]), the argument is irrelevant because the galactic field is weak and hence geons are *a priori* out of the question, even if they were viable in principle.

With regard to the issue of gauge, it was argued in [20] that asymptotically flat solutions are unattainable with a lead-off  $G^{1/2}$  order metric component. However, we have shown that they are readily attainable in conjunction with the physically desirable  $N_z$  discontinuity and are approximately attainable with the smoothed fine-tuned solution discussed above. Moreover, they are precisely attainable when

an essential singularity is invoked<sup>27</sup>. A key point is that the equations have an inherent non-linearity as a result of the fact that the metric components are of different orders and the different orders are a necessary consequence of the problem being a gravitationally bound one.

In [25], the author brings up the covariant vorticity and (vanishing) shear tensors for the rotating dust and poses the latter characteristic as being inconsistent with a galaxy that has differential rotation. However, a rotating dust cloud cannot physically rotate rigidly as does a disk of steel which has internal stresses. The answer to [25] is that the vanishing *covariant* shear is analogous to the vanishing *covariant* acceleration of a freely moving particle. In the case of the latter, it is only under very special conditions that the motion will be one of constant velocity. The generic motion will be conical or more complicated. This could have been recognized in [25] where the correct *differential* local angular velocity  $cN(r, z)/r^2$  is displayed. Also in [25], when the author chooses a solution for which the  $N$  function is taken to be zero at order  $G^{1/2}$ , he is being inconsistent with the demand that this is a gravitationally bound problem with rotation. Finally this author treats the transformation  $\phi \rightarrow \bar{\phi} = \phi + \omega(r, z)t$  as a ‘global’ transformation to the ‘co-moving frame’. However it is the original coordinate set that constitutes the co-moving frame and moreover, this transformation has value strictly as a local transformation.

The authors of [18] arrive at our equations (6), (7) (with  $w$  set to zero) apart from the exponential  $\nu$  factor which they later note can be taken to be a constant scaling factor and find the same order of magnitude reduction of galactic mass that we had found [1] starting from their exact solution class. This provides some vindication for our analysis. It should be noted that their scaling factor is actually incorporated in our solutions within the computed amplitudes of our basis expansion functions. To be particularly noted in [18] is that their solution class is fine-tuned as the density gradient is precisely zero at  $z = 0$ . The price that is paid to achieve this degree of smoothness is the incorporation of an axial singularity. These authors justify the singularity by identifying it as a jet. While jets are observed in various galaxies in their formative stages, they are not known to be present in the essentially stationary galaxies that are being modeled with this class.

A detailed analysis of the exact van Stockum [11] spacetime is provided in [28] from which the authors derive and transfer supposed restrictions onto our work. However in doing so, they miss the point that we are analyzing in generality the *weak-field* stationary axially symmetric dust spacetimes and hence restrictions

---

<sup>27</sup>This was almost achieved in [18]. Their axis singularity prevented global asymptotic flatness. However, exact solutions with compactified singularities of the Weyl type are likely to rectify this deficiency.

derived on an exactness basis from some particular solution are not relevant to us. Our solutions are approximate, with sufficient accuracy for the physical situation at hand.

Moreover, we have now considered various velocity fall-off scenarios beyond the HI regions and have extended our rotation curves to match these assumed fall-offs.<sup>28</sup> These are shown in figure 11. To accommodate this expanded region, this requires a completely new and enlarged set of parameters from those displayed in the Tables to follow the relatively flat region and then merge into the fall-off region. It is to be noted that since the velocity continues to be constructed in the form of (17), there is continuity of the curve and its derivatives apart from the value at precisely  $z = 0$  discussed previously. The kink in figure 11 is only apparent, arising from the practical need to fit the subtle transition into a compressed graph.

From (11), we see that the density vanishes when  $N_r$  and  $N_z$  are both zero, i.e. when  $N$  is a constant. Also, from (14), when  $N$  is a constant, the velocity falls as  $1/r$ . Therefore, at first glance one might believe that by choosing the continued velocity curves beyond the HI region in the form  $A_0/r$ , one would be tracking  $r$  into the vacuum, identifying  $N$  with a constant  $A_0$  and hence accumulating no further mass. However, while in plotting rotation curves at a given  $z$ , it is only a net independence in  $r$  for the  $N$  function that is required to give an  $A_0/r$  fall-off in  $V$ . The  $z$  dependence in the  $N$  function can still be present. Thus, the density will still not be zero and mass will still be accumulated as one tracks in the radial direction.<sup>29</sup> Faster fall-off rates with  $r$  would improve the trend towards vacuum further. Slower fall-offs such as of the form  $1/\sqrt{r}$  which might be suggested from Newtonian gravity are clearly not adequate to merge towards vanishing density.<sup>30</sup> It is also not necessary since we are basing our analysis on the preferred theory of gravity, namely general relativity. The challenge is to find a general relativistic solution that merges properly into near vacuum and we have met that challenge.

We display the accumulated mass for the Milky Way in a highly extended cylindrical volume of 300 Kpc in size in figure 12. It is to be noted that even assuming a Newtonian-like fall-off of the form  $1/\sqrt{r}$ , there is a far less amount of accumulated mass up to a radius of ten times the visible radius than is envisaged

---

<sup>28</sup>It is to be noted that this is in keeping with our desire to work with globally dust models, thus avoiding transition issues for the metric and its derivatives in going from dust to total vacuum. Also to be stressed is that the points beyond the HI region are not based upon observed data but rather are artificially imposed to induce smooth matter fall-offs of various forms.

<sup>29</sup>This is evident in Figure 12.

<sup>30</sup>A fall-off of the form  $1/\sqrt{r}$  would be appropriate to impose for test particles in the field of a massive body such as is the case in the solar system. However, here we have seen that in the case of a continuous gravitationally bound source, general relativity presents a dynamical system with behavior that does not match the Newtonian picture.



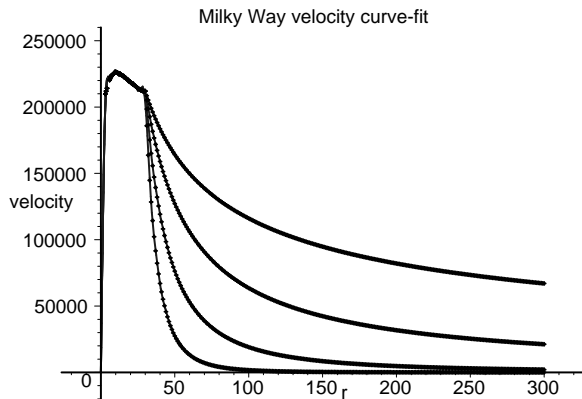


Figure 11: Beyond the HI region, the velocity can be modeled in many different manners: here  $V \propto 1/\sqrt{r}$ ,  $V \propto 1/r$ ,  $V \propto 1/r^2$  and  $V \propto 1/r^4$  are illustrated.

by the use of Newtonian as opposed to general relativistic galactic dynamics. An even slower accumulation of mass is seen for the  $1/r$  fall-off. For such a fall-off, the accumulated mass is approximately  $35 \times 10^{10} M_{\odot}$  at a radius of 300 Kpc and a linear extrapolation to  $r=900$  Kpc yields a value of  $39.2 \times 10^{10} M_{\odot}$ , a very modest increase in comparison to Newtonian modeling. Moreover, the faster fall-offs of  $1/r^2$  and  $1/r^4$  yield very minor mass increases out to very large radii as can be seen in figure 12.<sup>31</sup>

This fortifies our contention that general relativity obviates the need for overwhelmingly dominant massive halos of exotic dark matter.

It is to be noted that our models are *globally* dust<sup>32</sup> and therefore there is no basis for a matching with the vacuum Kerr metric asymptotically. Our models are asymptotically flat with a well-defined mass. The Tolman integral dictates the value of this mass and since there is no stress and the fields are weak, the Tolman mass to lowest order is simply given by the coordinate volume integral of the density.

In [29], the observed solar neighborhood density data are compared with the values given by our model. These authors find that our density is less by a factor of approximately six. Firstly, it is to be noted that there are considerable error

<sup>31</sup>Note from this figure that the accumulated mass at 30 Kpc is approximately the same for the various fall-off scenarios as well as the value stated in Section 3 where we used only 10 parameters and where we did not focus on the behavior of the model beyond the 30 Kpc edge of the HI region.

<sup>32</sup>We make this choice for the composition and distribution of the matter for the purpose of mathematical simplicity.

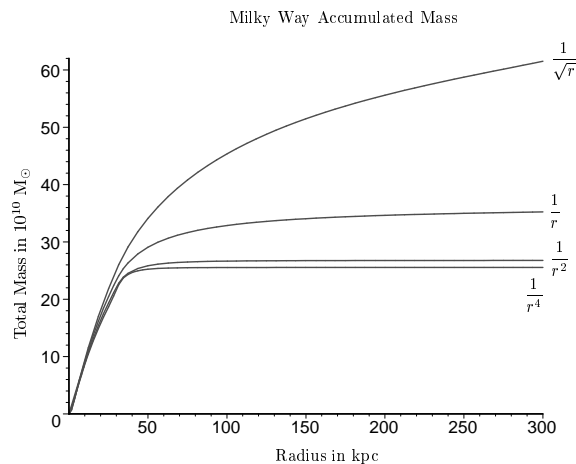


Figure 12: The Milky Way’s accumulated mass as a consequence of velocity faall-off beyond the HI region.

bars on their data and it is possible that our neighborhood could be one of enhanced density. Secondly, it must be emphasized that our model is adjusted in the simplest terms to account for the overall mean velocity distribution with a mere ten parameters.<sup>33</sup> This scant input can hardly be expected to account for the distribution of hundreds of billions of stars and their motions. This is beyond the capacity of even Newtonian theory let alone general relativity. By necessity, great simplifications are necessary in practice. Moreover, as additional support for our model having the correct overall characteristics, our integrated density over the visible region falls within predicted limits.

Even if one were to assume a logical basis for making their comparison between local observed data and our globally derived very approximate data, it should be noted that the vertical distribution of observed stars in the local galactic disk has a sharp peak [30]. This fits in well with the presence of a density gradient discontinuity in our models. Moreover, it should be noted that for mathematical tractability, we have assumed that the density peaks all occur at  $z = 0$ . However, there will naturally be some variation in the location in  $z$  for these peaks. Due to the rapid decline in density, there will be large local variations in density and therefore the criticisms in [29] about our distributions are further seen to be inappropriate.

---

<sup>33</sup>Even with the enlarged parameter set used to model the asymptotic fall-off, the parameter input is still quite modest.

In [31], the author models the galaxy via Newtonian physics with a surface mass layer. Clearly, given the freedom to impose the properly adjusted internal stresses, virtually any kind of approximate velocity distribution can be simulated. This is inadequate for the problem at hand on two counts: firstly, a good model should be stress-free (i.e. purely free-fall gravitationally driven) and secondly, the point is to develop an extended *volume* distribution and hence more akin to reality. This is what we have set out to do and this, within general relativity, the preferred theory of gravity. Moreover, there is the suggestion, sometimes reiterated by others, that we claim to have modeled galaxies without any dark matter, this in spite of the fact that we have explicitly referred to dead stars, neutron stars, etc. as dark matter constituents of galaxies and we have presented mass-to-light ratios. What we are questioning is the existence of *exotic* dark matter, the supposed constituent of the massive halos 5 to 10 times the traditionally computed mass that are said to surround galaxies, matter that has no known counterpart to the matter that physicists identify in labs and particle accelerators. Our approach is in keeping with the spirit of Occam.

In [32], the authors fault our models as extended constructs that indicate enormous quantities of mass beyond the HI regions. This is a useful point of criticism in that we had not investigated earlier the asymptotic consequences of the particular parameter sets that we had chosen to model the observed rotation curves.<sup>34</sup> However, in this paper, as first reported in [3], we assure more realistic fall-off scenarios<sup>35</sup> and we find that the accumulated mass profiles indicate that most of the mass of a galaxy is confined fairly close to the region of the visible disk with *modest* accumulations of mass beyond this region. General relativity achieves this with a pressure-free fluid model, unlike Newtonian gravity.

The comments above referring to [28] apply also to [33]. Moreover, as we have reported at various seminars in June/July 2006 and as described above, we have avoided the complications of merging from the dust regions to vacuum by dealing with models that are globally dust. Since the dust in our models become extremely diffuse with distance, the physical distinction between having the global dust and the vacuum is inconsequential. Also to be noted is that since the  $N$  function is ultimately connected to solutions of the Laplace equation, there will necessarily be a singularity of some form present. It is quite acceptable if it is the right kind of

---

<sup>34</sup>Note however that their argument that mass accumulates linearly in  $r$  is faulty as a generalization. With the correct combination of parameters, the term that would lead to such an accumulation can be eliminated. Our examples in which we achieve minimal accumulation, provide the direct proof that this is the case.

<sup>35</sup>It is to be noted that in so doing, while the expansion parameters are no longer the same as in the earlier sets, we have determined that the net physical effects are of insignificant difference within the observed matter distribution in the two approaches.

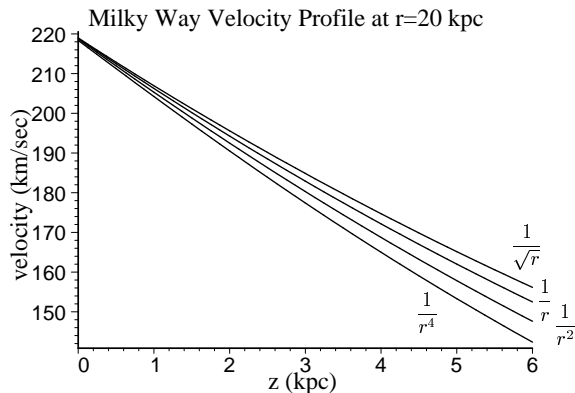


Figure 13: Velocity dispersion at  $r = 20$  kpc for the Milky Way.

singularity and in our construction it is the case, modeling the physically desirable density gradient discontinuity.

In an interesting approach from a very different direction, Lusanna [19] has pointed to relativistic inertial effects that do not have a Newtonian limit counterpart. He has suggested that in the weak field limit, these effects could match our results.

## 5 Velocity Dispersion Test

Clearly it is important to approach the exotic dark matter issue in as many ways as possible. After all, from a purely formal point of view, general relativity should be able to model vastly extended distributions of pressure-free fluids in rotation. In this vein, we have constructed a test in principle that relies upon data in the *visible/HI* regime thus making it particularly useful. When we examine Figure 12, we see that different constructed velocity fall-off profiles beyond the HI region imply different mass accumulations in those external regions. Carrying these back with continuity into the visible/HI region, we find that the extent of the velocity dispersion as we track curves at different non-zero  $z$  values depends on the assumed external velocity profile fall-off. (See, for example, Figure 13.)

Thus, it is our request to our astronomical colleagues to kindly provide us with the data for rotation curves in planes of different  $z$  values. With sufficient data, it should be possible, at least in principle, to provide limits on the extent of extra matter that might lie outside of the visible/HI region.

## 6 Concluding Comments

One might be inclined to question how this large departure from the Newtonian picture regarding galactic rotation curves could have arisen since the planetary motion problem is also a gravitationally bound system and the deviations there using general relativity are so small. The reason is that the two problems are very different: in the planetary problem, the source of gravity is the sun and the planets are treated as test particles in this field (apart from contributing minor perturbations when necessary). They respond to the field of the sun but they do *not* contribute to the field. By contrast, in the galaxy problem, the source of the field is the combined rotating mass of all of the freely-gravitating elements themselves that compose the galaxy.

We have seen that the non-linearity for the computation of density inherent in the Einstein field equations for a stationary axially-symmetric pressure-free mass distribution, even in the case of weak fields, leads to the correct galactic velocity curves as opposed to the incorrect curves that had been derived on the basis of Newtonian gravitational theory. Indeed the results were consistent with the observations of velocity as a function of radius plotted as a rise followed by an essentially flat extended region and no halo of exotic dark matter with multiples of the normally computed galactic mass was required to achieve them. The density distribution that is revealed thereby is one of an essentially flattened disk without an accompanying overwhelmingly massive vastly extended dark matter halo. With the “dark” matter being associated with the disk which is itself visible, it is natural to regard the non-luminous material as normal baryonic matter.

It is unknown how far the galactic disks extend. More data points beyond those provided thus far by observational astronomers would enable us to extend the velocity curves further. We have made simplifying assumptions for various velocity fall-off scenarios and we have seen that these can readily yield a picture of galactic structure devoid of huge extended very massive halos of exotic dark matter.

Of particular interest is that we have within our grasp a criterion for determining the extent, if of any significance, of extra matter beyond the visible and HI regions of a galaxy. It is possible in principle to determine this with data solely *within* the visible/HI region by plotting the velocity dispersion of rotation curves for various  $z$  values. This is an attractive area for future research.

Nature is merciful in providing one linear equation that enables us by superposition to model disks of variable density distributions. This opens the way to studies of other sources and with further refinements. It is to be emphasized that what we have taken is a first step, a general relativistic as opposed to a Newtonian analysis at the galactic scale. It will be of interest to extend this general relativistic-

tic approach, with the hitherto neglected consideration of non-linearities, to the other relevant areas of astrophysics with the aim of determining whether there is any scope remaining for the presence of any exotic dark matter in the universe. For example, at the scale of clusters of galaxies, the virial theorem of Newtonian physics is used. However, such a system, albeit now chaotic, can again be viewed as a continuum of free-fall matter as was the case for the galactic scale. Indeed at the scale of individual galaxies as units within the cluster, the motions comprise a multitude of randomly oriented free-fall-rotations . While the chaotic nature of these rotations within a cluster might have the effect of minimizing or even erasing the kind of phenomenon that we have witnessed in the systematic rotation of an individual galaxy, it might be otherwise. Since general relativity was seen to make such a difference in the case of the galactic scale, clearly it is necessary to analyze the scale of the clusters anew.

The scientific method has been most successful when directed by Occam's razor, that new elements should not be introduced into a theory unless absolutely necessary. If it should turn out to be the case that the observations of astronomy can ultimately be explained without the addition of new exotic dark matter, this would be of considerable significance.

#### **Acknowledgments**

We thank our many colleagues for their interest in our work, their advice and criticism. This work was supported in part by a grant from the Natural Sciences and Engineering Research Council of Canada.

## **A Appendix**

The coefficients for

$$N(r, z) = - \sum_{n=1}^{10} C_n k_n r e^{-k_n |z|} J_1(k_n r)$$

are tabulated in Tables 1 to 4 with  $r$  and  $z$  in Kpc. The velocity in m/sec is given by

$$V(r, z) = \frac{3 \times 10^8}{r} N(r, z)$$

and the density in kg/m<sup>3</sup> is given by

$$\rho(r, z) = 5.64 \times 10^{-14} \frac{(N_r^2 + N_z^2)}{r^2}$$

$-C_n k_n$	$k_n$
0.0012636497740	0.06870930165
0.0004520156256	0.15771651740
0.0001785404942	0.24724936890
0.0002946610499	0.33690098400
0.0000103378815	0.42659764880
0.0002127633340	0.51631611340
-0.0000221015927	0.60604676080
0.0001346275993	0.69578490080
-0.0000123824930	0.78552797510
0.0000666973093	0.87527447050

Table 1: Curve-fitted coefficients for the Milky Way

## References

- [1] F. I. Cooperstock and S. Tieu, astro-ph/0507619.
- [2] F. I. Cooperstock and S. Tieu, astro-ph/0512048.
- [3] F. I. Cooperstock and S. Tieu (22nd Pacific Coast Gravity Meeting, KITP, Santa Barbara, California, 2006).
- [4] F. I. Cooperstock and S. Tieu, Mod. Phys. Lett. A. **21**, 2133 (2006).
- [5] J. Binney and S. Tremaine, *Galactic Dynamics* (Princeton University Press, Princeton, N.J., 1987).
- [6] M. Milgrom, Ap. J. **270**, 365 (1983).
- [7] M. Milgrom and J. D. Bekenstein, Ap. J. **286**, 7 (1984).
- [8] J. D. Bekenstein, *Developments in General Relativity, Astrophysics and Quantum Theory* (Eds. F. I. Cooperstock, L. P. Horwitz and J. Rosen, IOP Publishing Ltd, Bristol, England, 1990).
- [9] J. R. Brownstein and J. W. Moffat, astro-ph/0506370.
- [10] L. Mestel, MNRAS **126**, 553 (1963).
- [11] W. J. van Stockum, Proc. R. Soc. Edin. **57**, 135 (1937).
- [12] W. B. Bonnor, J. Phys. A: Math. Gen. **10**, 1673 (1977).
- [13] J. M. Bardeen, Astrophys. J. **162**, 71 (1970).
- [14] F. I. Cooperstock, S. Jhingan, P. S. Joshi and T. P. Singh, Class. Quantum Grav. **14**, 2195 (1997).

$-C_n k_n$	$k_n$
0.0011694103480	0.1093102526
0.0004356556836	0.2509126413
0.0003677376760	0.3933512687
0.0001484103801	0.5359788381
0.0000837048346	0.6786780777
0.0000414084713	0.8214119986
0.0000429277032	0.9641653013
0.0000550130755	1.1069305240
0.0000238560073	1.2497035970
0.0000129841761	1.3924821120

Table 2: Curve-fitted coefficients for NGC 3031

- [15] S. M. Kent, *Astron. J.* **93**, 816 (1987).
- [16] T. S. van Albada, J. N. Bahcall, K. Begeman and R. Sancisi, *Ap. J.* **295**, 305 (1985).
- [17] R. B. Tully and J. R. Fisher, *Astronomy and Astrophysics* **54**, 661 (1977).
- [18] H. Balasin and D. Grumiller, *astro-ph/0602519*.
- [19] L. Lusanna, *gr-qc/0604120*.
- [20] M. Korzynski, *astro-ph/0508377*.
- [21] D. Vogt and P. S. Letelier, *astro-ph/0510750*.
- [22] W. B. Bonnor, 2005 preprint.
- [23] D. Garfinkle, *Class. Quant. Grav.* **23**, 1391 (2006), *gr-qc/0511082*.
- [24] M. D. Maia, A. J. S. Capistrano and D. Muller, *astro-ph/0605688*.
- [25] D. J. Cross, *astro-ph/0601191*.
- [26] F. I. Cooperstock, V. Faraoni and G. P. Perry, *Int. J. Mod. Phys. D* **5**, 375 (1996).
- [27] G. P. Perry and F. I. Cooperstock, *Class. Quantum Grav.* **16**, 1889 (1999).
- [28] L. Bratek, J. Jalocho and M. Kutschera, *astro-ph/0603791*.
- [29] B. Fuchs and S. Phelps, *New Astron.* **11**, 608 (2006), *astro-ph/0604022*.
- [30] J. Holmberg and C. Flynn, *MNRAS* **313**, 209 (2000).
- [31] V. Kostov, *astro-ph/0604395*.



$-C_n k_n$	$k_n$
0.00093352334660	0.07515079869
0.00020761839560	0.17250244090
0.00022878035710	0.27042899730
0.00009325578799	0.3684854512
0.00007945062639	0.4665911784
0.00006081834319	0.5647207491
0.00003242780880	0.6628636447
0.00003006457058	0.7610147353
0.00001687931928	0.8591712228
0.00003651365250	0.9573314522

Table 3: Curve-fitted coefficients for NGC 3198

- [32] D. Menzies and G. J. Mathews, gr-qc/0604092.
- [33] T. Zingg, A. Aste and D. Trautmann, astro-ph/0608299.
- [34] C. R. Keeton, *Ap. J.* **561**, 46 (2001).
- [35] J. Winicour, *J. Math. Phys.* **16**, 1805 (1975).
- [36] J. C. N. de Araujo and A. Wang, *Gen. Rel. Grav.* **32**, 1971 (2000).
- [37] L. B. Ford, *Differential Equations* (McGraw-Hill, 1955).
- [38] L. Clewley, S. J. Warren, P. C. Hewett, M. Wilkinson and W. N. Evans, astro-ph/0310675.
- [39] M. Wilkinson and N. Evans, *MNRAS* **310**, 645 (1999).

$-C_n k_n$	$k_n$
0.0015071991080	0.0586542819
0.0003090462519	0.1346360514
0.0003960391396	0.2110665344
0.0001912008955	0.2875984009
0.0002161444650	0.3641687246
0.0000988404542	0.4407576578
0.0001046496277	0.5173569909
0.0000619051218	0.5939627202
0.0000647087250	0.6705726616
0.0000457420923	0.7471855236

Table 4: Curve-fitted coefficients for NGC 7331